

Shell effects on fission barriers of metallic clusters: A systematic description

Armando Vieira and Carlos Fiolhais

Departamento de Física, Universidade de Coimbra, 3000 Coimbra, Portugal

(Received 20 May 1997; revised manuscript received 30 October 1997)

We use the liquid drop model, with the stabilized jellium model, and the Strutinsky shell correction method [Nucl. Phys. A **95**, 420 (1967); **122**, 1 (1968)], with the two-center asymmetric deformed harmonic-oscillator potential, to evaluate fission barriers for three representative simple metal clusters (sodium, aluminum, and potassium). We obtain fission barrier heights as a function of size, charge, and mass asymmetry for all possible decay channels of doubly charged clusters with up to 30 atoms. We show how fragment deformations change the barrier height. For small sodium and potassium clusters we find good agreement of the fission barriers with molecular-dynamics calculations. The critical number (cluster size for which fission competes with evaporation) is correctly reproduced for doubly charged clusters of the three metals considered.

[S0163-1829(98)00808-X]

I. INTRODUCTION

The liquid drop model (LDM) is useful to understand the main trends of metal cluster fission. If we consider a charged simple metal cluster as a spherical liquid drop consisting of valence electrons in the field created by a positive background (jellium¹ or stabilized jellium,² which is essentially jellium corrected by introducing a constant potential inside the metal), there are two main competing terms: the surface energy, which tries to keep the system spherical, and the Coulomb energy, which tends to deform it. Fission is controlled by the fissibility x , which is half of the ratio between those two quantities. Assuming that the fission channel is determined by minimizing the heat of reaction, very asymmetric reactions are favored for small x and as x approaches unity, the Coulomb term becomes dominant and symmetric splitting prevails.

However, the decay channel is determined by the fission barrier rather than the heat of reaction. We studied in Ref. 3 fission barriers of metallic clusters using the LDM within the jellium model. In particular, we calculated the barrier height as a function of mass and charge asymmetry for different fissibilities. A good account of the experimental critical numbers (cluster sizes for which the evaporation energy is equal to the fission barrier) was made.

Quantal shell effects change the LDM heats of reaction: The channels with the more stable fragments become clearly the most favorable.^{4,5} These corrections to the liquid drop energy are essential for obtaining not only realistic heats of reaction but also good barrier heights. The shell correction method (SCM) is adequate to study complex quantal systems when more rigorous methods are useless, such as large or deformed nuclei or clusters, and has been systematically applied to nuclear fission with great success. In the SCM, shell corrections are evaluated replacing the effective potential "felt" by the valence electrons by a simpler, non-self-consistent potential.⁶ The total energy is obtained by adding these shell fluctuations to the smooth LDM energy. One advantage of the SCM is that it may be used, with little in-

crease of computational cost, for systems with arbitrary size and charge.

In a previous work,⁷ we used the SCM to study symmetric fragmentations of sodium clusters, concluding that shell corrections play a crucial role in shaping fission barriers and that the two-center harmonic oscillator is able to reproduce the major quantal oscillations. Yannouleas and Landman⁸ used recently the two-center asymmetric harmonic oscillator⁹ to study the influence of shell effects on a couple of sodium cluster decays. These authors have pointed out the importance of allowing for fragment deformations to obtain correct fission barriers. The present work is an extension of those studies aiming at systematically evaluating fission barriers for several charged metal clusters. We study fission barriers of double charged clusters of sodium, aluminum, and potassium containing up to 30 atoms. The barriers are calculated for all possible decay channels including independent ellipsoidal deformations of both fragments. We analyze the role of mass asymmetry and fragment deformations in the fission barriers.

The experimental information on the fission of charged clusters is scarce. Näher *et al.*¹⁰ determined critical numbers for a set of alkali-metal clusters ionized up to seven times. In addition to the critical numbers, we know the barrier heights of systems with a size close to N_c and the main decay channel. Bréchnignac *et al.*¹¹ measured barrier heights. Recently,¹² her group was able to determine the internal and the external fission barriers for charged metal clusters by measuring the decay rates and the kinetic energy of the emergent fragments. For systems with $N \approx N_c$ the fissibilities are moderate ($x \approx 0.5$),³ corresponding to very asymmetric reactions. The most favored decay channel, within the LDM, has then one small singly charged fragment. Shell corrections do not change this result. Therefore, symmetric fission, common in nuclei, is not expected and has not been observed in alkali-metal clusters. Notwithstanding, we will point out a small number of examples for which symmetric fission may be found due to the special stability of the fragments.

This work is organized as follows. In Sec. II we discuss briefly the liquid drop formula for charged spherical and de-

TABLE I. Liquid drop coefficients for the stabilized jellium model. The values for $a_s=4\pi r_s^2\sigma$ and $a_c=2\pi r_s\gamma$ are taken from Fiolhais and Perdew (Ref. 14). The values of c are from Vieira, Brajczewska, and Fiolhais (Ref. 4) (Al) and from Seidl and Brack (Ref. 16) (Na; these authors used jellium instead of stabilized jellium). The values of d_s are from Kiejna (Ref. 15).

Metal (r_s)	a_s (eV)	a_c (eV)	c	d_s (a.u.)
Na (3.93)	0.58	0.26	-0.082	1.27
Al (2.07)	0.87	0.65	-0.1	1.01

formed clusters and present the potential to be used in the SCM. In Sec. III we present results for barrier heights of doubly charged sodium, aluminium, and potassium clusters, with up to 30 atoms. The results of our calculations, for spherical as well as deformed fragments, are compared with molecular dynamics and experiment. The critical numbers are determined and compared with experiment. Section IV contains the conclusions, after further comparison with other theoretical results. A short report on some of these results appears in Ref. 13.

II. SHELL CORRECTION METHOD

A. Liquid drop model

For a *spherical* cluster with N valence electrons and z missing electrons, the LDM energy is (we use $l=c=\hbar=1$)

$$E_{\text{LDM}}(N, z) = a_v V + \sigma S + \gamma C + z \left(W + \frac{c}{R_0} \right) + (z)^2 a_{\text{Coul}}, \quad (1)$$

where $V = \frac{4}{3}\pi R_0^3$ is the volume ($R_0 = r_s N^{1/3}$ is the cluster radius, r_s being the density parameter), $S = 4\pi R_0^2$ is the surface, and $C = 2\pi R_0$ is half the mean curvature. The parameters a_v , σ , and γ are the volume, surface, and curvature coefficients for a neutral cluster (see Table I). The fourth term of Eq. (1) includes the work function W and its first-order size correction, so that the chemical potential is $\mu = -(W + c/R_0)$. The last term is the classical electrostatic energy, obtained under the assumption that the cluster is a perfect conductor: $a_{\text{Coul}} = 1/2(R_0 + d_s)$. The parameter d_s accounts for the charge spill-out effect: The position of the excess charge lies on a radial centroid displaced d_s from the jellium surface.

For a *deformed* cluster, Eq. (1) holds with the following modifications: (i) $S = \int dA$; (ii) $C = \frac{1}{4} \int (1/R_{\min} + 1/R_{\max}) dA$, with R_{\min} and R_{\max} the principal radii of curvature at a point of the surface; (iii) since the correction to the work function is unknown for deformed systems, we have used an interpolation formula between the limits c/R_0 and $c(1/R_1 + 1/R_2)$, where R_1 and R_2 are the radii of the final spherical fragments; (iv) a_{Coul} is calculated numerically assuming always that the excess charge is distributed on the surface (we follow Ref. 17 to obtain the distribution of charge). Volume is conserved during deformation and fragmentation.

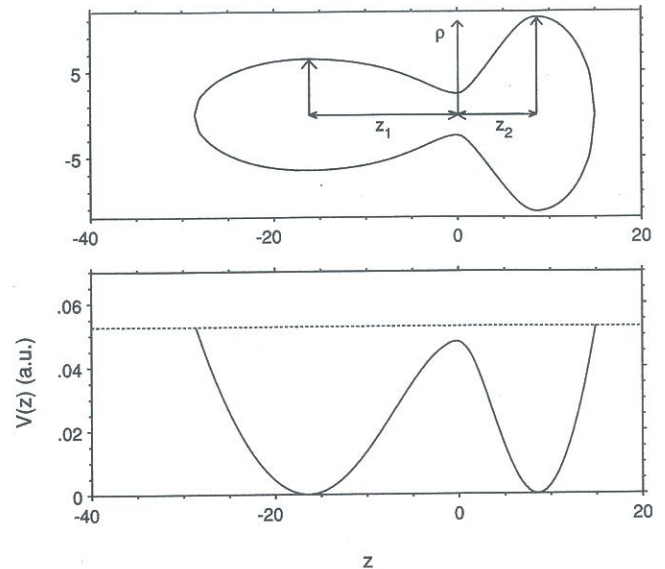


FIG. 1. Top: a cluster shape described by Eq. (7) with $d=25$, $\delta_1=2.0$, $\delta_2=0.5$, and $\lambda=1.52$. Bottom: the z dependent potential given by Eq. (4).

The LDM gives a good average of the Kohn-Sham energies of spherical jellium clusters, even for very small clusters, neutral¹⁸ as well as charged.⁴ If the spherical symmetry is broken, the agreement of the LDM with quantal results is even better since the shell fluctuations becomes less pronounced.¹⁹

For very asymmetric reactions, the usually neglected curvature term, the work function size correction, and the spill-out effect may be relevant to the LDM fission barriers. Let us estimate the contribution of these terms to the heat of the reaction $[N]^{2+} \rightarrow [N-p]^+ + [p]^+$ for large N and small p . The curvature term contribution is $a_c p^{1/3}$. Additionally, we get terms like

$$\frac{c}{r_s} p^{-1/3} \quad (2)$$

and

$$-\frac{d_s}{2r_s^2} p^{-2/3}. \quad (3)$$

For Na_{200}^{2+} with $p=3$, we obtain $0.74 + (-0.39) + (-0.03) = 0.32$ eV, with the successive terms associated with a_c , c , and d_s , respectively. We remark that in the LDM we always refer to electronic density shapes, which do not need to agree with positive background shapes, when using jellium type models for the ions.

B. Potential

The two-center asymmetric harmonic-oscillator potential (Fig. 1), with centers at $z_1 < 0$ and $z_2 > 0$, is

$$V(\rho, z) = \begin{cases} \frac{1}{2} \omega_{\rho_1}^2(z) \rho^2 + \frac{1}{2} \omega_{z_1}^2(z - z_1)^2 + V_{\text{neck}}(z) + U(\mathbf{l}^2), & z < 0 \\ \frac{1}{2} \omega_{\rho_2}^2(z) \rho^2 + \frac{1}{2} \omega_{z_2}^2(z - z_2)^2 + V_{\text{neck}}(z) + U(\mathbf{l}^2), & z > 0. \end{cases} \quad (4)$$

The frequency associated with the coordinate ρ , $\omega_\rho(z)$, interpolates smoothly between the frequencies in the ρ direction on the left-hand side ω_{ρ_1} and the right-hand side ω_{ρ_2} :

$$\omega_\rho(z) = \sqrt{\omega_{\rho_i}^2 + \alpha_i [(z - z_i)^2 + \xi_i (z - z_i)^4 \theta(|z| - |z_i|)]}, \quad (5)$$

where α_i and ξ_i are parameters to be determined and θ is the step function. The term V_{neck} , which is included to smooth the cusp in the origin, has the form

$$V_{\text{neck}} = \frac{1}{2} \xi_i \omega_{z_i}^2 (z - z_i)^4 \theta(|z| - |z_i|). \quad (6)$$

The cluster shape corresponding to the single-particle potential is obtained by assuming that the surface is an equipotential with value $V_0 = \frac{1}{2} \omega_0^2 R_0^2$ (see Fig. 1):

$$\rho(z) = \frac{\sqrt{\omega_0^2 R_0^2 - \omega_{z_i}^2 (z - z_i)^2 - \xi_i \omega_{z_i}^2 (z - z_i)^4 \theta(|z| - |z_i|)}}{\omega_\rho(z)}. \quad (7)$$

The quantity

$$\omega_0 = \epsilon_F / (3N)^{1/3}, \quad (8)$$

with ϵ_F the Fermi energy, is the corresponding harmonic-oscillator frequency. The shapes obtained are ellipsoids (prolate or oblate) connected by a smooth neck (see Fig. 1).

The values of ξ_i and α_i are obtained by imposing the continuity condition on $\rho(z=0)$ and $V(\rho, z=0)$ and on their first derivatives $d\rho(z)/dz|_{z=0}$ and $dV(\rho, z)/dz|_{z=0}$. The results are

$$\xi_i = -\frac{1}{2z_i^2}, \quad (9)$$

$$\omega_{z_1} z_1 = \omega_{z_2} z_2, \quad (10)$$

$$\omega_{\rho_1}^2 + \frac{1}{2} \alpha_1 z_1^2 = \omega_{\rho_2}^2 + \frac{1}{2} \alpha_2 z_2^2. \quad (11)$$

When $d = z_2 - z_1 \rightarrow \infty$, we should get two independent Nilsson potentials, i.e., $\alpha_i \rightarrow 0$ for large z_i ($i=1,2$). Using $\omega_\rho^2(z=0) = \frac{1}{2}(\omega_{\rho_1}^2 + \omega_{\rho_2}^2)$, we obtain

$$\alpha_i = \frac{1}{z_i^2} (\omega_{\rho_1}^2 - \omega_{\rho_2}^2). \quad (12)$$

These continuity conditions together with the volume conservation condition lead to four independent shape parameters: the distance between the two semiellipsoids $d = z_2 - z_1$, the deformation of each fragment $\delta_i = \omega_{\rho_i} / \omega_{z_i}$ ($i=1,2$), and $\lambda = \omega_{\rho_1} / \omega_{\rho_2}$, which is related to the mass asymmetry parameter $\alpha = p/N$ by

$$\lambda = \left[\frac{\delta_1 (1 - \alpha)}{\delta_2} \right]^{1/3}. \quad (13)$$

The Schrödinger equation for the potential of Eq. (4) is separable in the coordinates ρ and z by expressing the wave function as $|n_z N_\rho\rangle = |n_z\rangle |N_\rho\rangle$, with n_z and $N_\rho = 2n_\rho + |m|$ the quantum numbers in the z and ρ directions, and $|n_z\rangle$ and $|N_\rho\rangle$ the respective wave functions. For the symmetry axis, the wave functions and respective eigenvalues ϵ_z are obtained by numerical integration. The energy spectrum is given by [neglecting the $U(\mathbf{l}^2)$ term]

$$E_{n_z, n_\rho, m} = \epsilon_z + \omega_\rho (N_\rho + 1), \quad (14)$$

where $\omega_\rho = (\omega_{\rho_1} + \omega_{\rho_2})/2$.

To this energy we add a contribution due to the ϵ term

$$U(\mathbf{l}^2) = -U_0 \omega_0 (\mathbf{l}^2 - \langle \mathbf{l}^2 \rangle_n). \quad (15)$$

This decreases the degeneracy of the harmonic oscillator by favoring the electrons with higher angular momentum. The effect of this term is calculated following Ref. 20, with the parameter $U_0 = 0.04$ adjusted to mimic the energy-level structure of the self-consistent spectrum obtained from the spherical jellium model.

C. Shell corrections

Shell corrections arise because of fluctuations in the actual distribution of single-particle levels with respect to a smooth distribution. Strutinsky has proposed a technique to extract an average total energy from a given single-particle energy spectrum ϵ_i ($i=1,2,\dots$).⁶ The shell correction is given by

$$E_{SC} = \sum_{i=1}^N \epsilon_i - \bar{E}, \quad (16)$$

where \bar{E} is a conveniently defined average energy. The potential energy is the sum of the LDM term and the shell correction

$$E = E_{LDM} + E_{SC}. \quad (17)$$

Let us estimate the shell corrections effect on the fission barrier. Using the simple harmonic-oscillator potential, the largest shell correction for a spherical cluster with N valence electrons is $E_{SC} = \epsilon_F N^{1/3}$. Shell corrections are more important for high-density metals, such as aluminum ($\epsilon_F \sim 1/r_s^2$). On the other hand, for the spherical potential with infinite walls, we have $E_{SC} = \epsilon_F N^{-1/3}$. Since the effective potential "felt" by the valence electrons in the cluster is intermediate between these two potentials, we expect that, for a given metal, shell corrections do not depend very much on cluster size.

For $z = \gamma = 0$, the LDM barrier height is

$$E_b = a_s [\alpha^{2/3} + (1 - \alpha)^{2/3} - 1] N^{2/3}. \quad (18)$$

We compare now the shell correction with this quantity

$$\Delta E_{SC} = \frac{E_{SC}}{E_b} \sim \frac{\epsilon_F}{a_s} \frac{N^{-2/3}}{[\alpha^{2/3} + (1 - \alpha)^{2/3} - 1]}. \quad (19)$$

We conclude that (i) shell corrections are essential for small clusters, (ii) ΔE_{SC} decreases with $N^{-2/3}$ for symmetric fission, and (iii) for a given fragmentation channel p , ΔE_{SC} goes with $p^{-2/3}$ when $N \rightarrow \infty$, so that shell corrections may be important even for the fission of big clusters.

We may use Eq. (19) to compare shell corrections of clusters and nuclei. For typical values $a_s \approx 1$ eV and $\epsilon_F \approx 3$ eV for clusters and $a_s \approx 18$ MeV and $\epsilon_F \approx 8$ MeV for nuclei, we find that, for a given number of particles, ΔE_{SC} may be about 6 times higher for clusters than for nuclei.

III. RESULTS

To test the SCM, we compare in Fig. 2 the barrier for the reaction $\text{Na}_{10}^{2+} \rightarrow \text{Na}_7^+ + \text{Na}_3^+$ calculated with the SCM with that obtained by Barnett *et al.*²¹ using quantal molecular dynamics (MD) in the local-spin-density approximation. The agreement is rather good. In the same figure, we also compare our results with those obtained by Rigo *et al.*²² for the reaction $\text{Na}_{24}^{2+} \rightarrow \text{Na}_{21}^+ + \text{Na}_3^+$ by solving the Kohn-Sham equations for two intersecting jellium spheres. The two deformation energies agree, having their minimum and maximum at similar positions.

Encouraged by these agreements, we proceed to study systematically the barrier heights of several small clusters decaying in all possible channels. We consider the potential energy of Na_{18}^{2+} as a function of the distance d between fragments and the fission channel p (Fig. 3). This system is interesting since emission of the magic piece Na_3^+ competes with symmetric fission in two magic pieces.

We present the result of two calculations. In the first we keep the mother and the daughter clusters with a spherical shape, fixing the deformation parameters to be $\delta_1 = \delta_2 = 1$ (SCM-sph). In the second case (SCM-def) we consider the four degrees of freedom (d , λ , δ_1 , and δ_2). The determination of the fission path when the energy depends on more

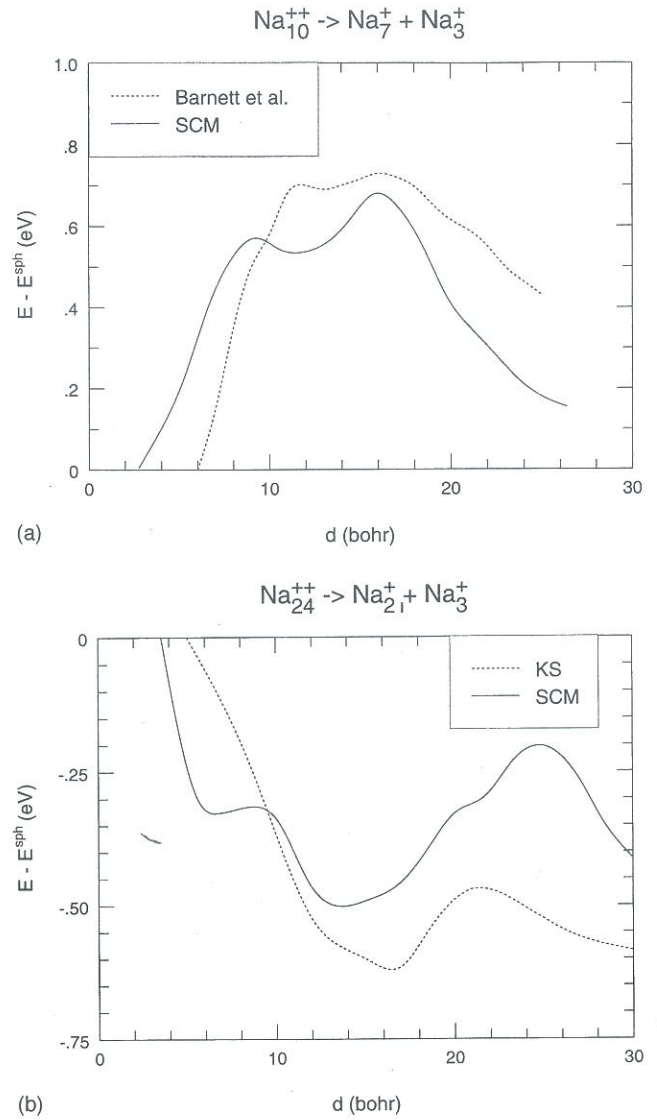


FIG. 2. (a) Comparison of SCM results with molecular dynamics for the reaction $\text{Na}_{10}^{2+} \rightarrow \text{Na}_7^+ + \text{Na}_3^+$ (Ref. 21). In the SCM both the mother and the daughter clusters are kept spherical for both reactions. (b) Comparison of the fission barrier obtained in the SCM with Kohn-Sham (KS) results for deformed jellium (Ref. 22).

than three parameters is a difficult task. Instead, we fix the distance d and the asymmetry λ and choose δ_1 and δ_2 minimizing the total energy. Doing this, we are assuming that for a given separation between unequal fragments the system adjusts instantaneously its shape to the lowest-energy configuration (adiabatic approximation). However, this procedure does not guarantee that we are following the path with the lowest-energy barrier among all possibilities in the multidimensional landscape.

In the first case, the channel $p=2$ has a minimal energy just before reaching the scission point ($d \approx 23$ bohr). However, as the system crosses this point, a sudden energy increase occurs due to the Coulomb self-energy of the smaller fragment. The channel with the lowest barrier corresponds to the splitting in two magic fragments ($p=9$). In the second case, the channel $p=6$ has the lowest barrier (0.12 eV).

Table II shows the barrier heights corresponding to the decays $\text{Na}_N^{2+} \rightarrow \text{Na}_{N-p}^+ + \text{Na}_p^+$, with $6 \leq N \leq 30$, for the

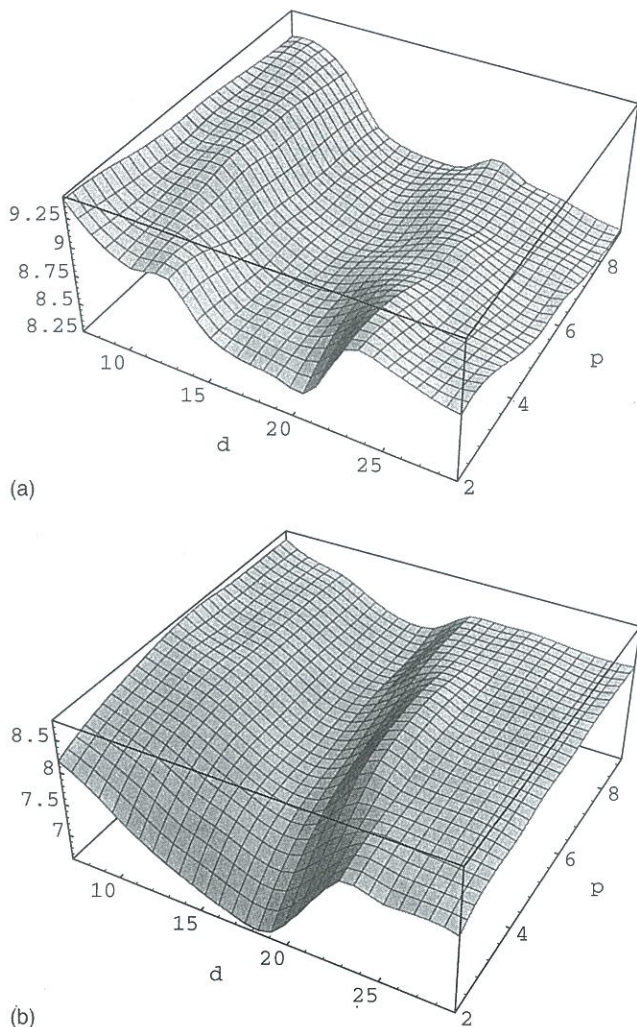


FIG. 3. (a) Potential energy for the system Na_{18}^{2+} as a function of the distance d between the fragments and the fission channel p , keeping the fragments spherical (SCM-sph). (b) Same as (a) but minimizing the energy with respect to the parameters δ_1 and δ_2 (SCM-def). The energy is in eV.

most favorable channel p , for several cluster sizes (see Fig. 1 of Ref. 13). We conclude that shell effects are quite strong and that spherical and deformed approaches give rather distinct results. For $N \leq 10$, the LDM barrier vanishes and the barrier is exclusively due to electronic shell effects. The LDM predicts that symmetric fission is favored for $x > 0.57$,³ corresponding to $N < 21$. This prediction is partially corroborated by our SCM-def results since we find fission to be symmetric for $N = 6, 8, 12, 14, 16$, and 18 .

The most favorable channel has, in general, a magic, or near-magic piece ($p = 3, 9$, or 21), in agreement with the heat of reaction analysis.⁵ However, the channel $p = 3$ is the most favored only for a small number of systems. The very asymmetric channel $p = 2$, not predicted on the basis of the heats of reaction, is the most favored for small clusters in the SCM-sph. For $6 \leq N \leq 12$, the favored decay channel in our calculations is not always $p = 3$, as indicated by Barnett *et al.*,²¹ and, for $N = 6$ and 7 , the SCM-sph predicts spontaneous fission. The most favored channel for the decay of

TABLE II. Barrier heights E_b (in eV) for the most favorable decay channel p of Na_N^{2+} and Al_N^{2+} clusters obtained with the SCM with spherical and deformed fragments.

N	Na_N^{2+}		Al_N^{2+}	
	Spherical E_b	Deformed p	Spherical E_b	Deformed p
2			0.00	1
3			1.78	1
4			1.76	1
5			1.76	1
6	0.00	3	0.23	3
7	0.00	3	1.05	1
8	0.11	2	1.30	1
9	0.32	2	1.31	1
10	0.54	2	1.40	1
11	0.29	2	1.17	1
12	0.42	2	2.55	1
13	0.46	2	1.75	5
14	0.46	2	0.88	5
15	0.59	2	1.22	2
16	0.64	5	1.09	2
17	0.34	5	1.22	2
18	0.25	9	1.48	2
19	0.26	6	1.78	1
20	0.27	5	1.66	1
21	0.37	3	2.67	8
22	0.53	4		
23	0.38	3		
24	0.34	2		
25	0.25	2		
26	0.26	2		
27	0.46	2		
28	0.74	2		
29	0.76	4		
30	0.77	3		

Na_{27}^{2+} is $p = 4$ (SCM-def) or $p = 2$ (SCM-sph), close to the result $p = 3$ of Ref. 23.

For both spherical and deformed versions of the SCM, initial clusters with a magic number of electrons, such as $N = 10$ and 22 , are particularly stable with respect to fission. For these clusters, we find that the SCM-def barrier is higher than the SCM-sph one. This is due to the fact that, in the path to fission, the system goes through a configuration with lower potential energy. By virtue of their special stability, these clusters are good candidates for the experimental study of the so-called rapid fission (characterized by charging cold clusters by photoionization).

The SCM-def gives rise, in general, to higher fission barriers than the SCM-sph, especially for $N \leq 16$ and $20 \leq N \leq 23$. This may be due to the deformation of nonmagic clusters, whose ground-state energies can be much lower than those of spherical ones. For $N = 28, 29$, and 30 the barrier is only slightly higher than the evaporation energy for spherical fragments. This fact agrees with experimental data from Bréchnignac *et al.*,²³ who detected a strong competition between fission and evaporation in that size range. The critical number for these clusters is $N_c = 27$ (SCM-def) or 28 (SCM-

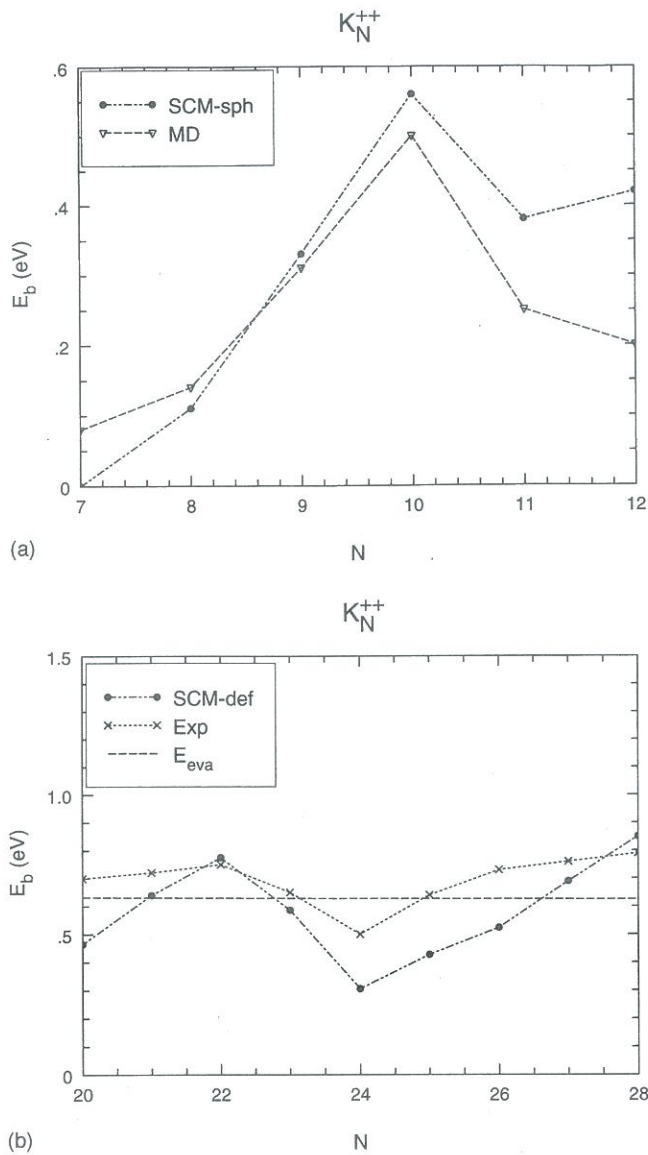


FIG. 4. (a) Fission barrier height of K_N^{2+} for the magic channel $p=3$ in the SCM with spherical fragments (SCM-sph), in comparison to the molecular-dynamics (MD) results of Bréchnignac *et al.* (Ref. 26). (b) Fission barrier heights for K_N^{2+} for the magic channel $p=3$ in the SCM with deformed fragments (SCM-def), in comparison to the experimental results (Expt.) (Ref. 27). E_{eva} denotes the LDM evaporation energy.

sph), in excellent agreement with the experimental value $N_c = 27 \pm 1$.¹⁰

Table II presents, in parallel with the results for sodium, the barrier heights for the decay of doubly charged aluminum clusters (see Fig. 2 of Ref. 13). To simplify the notation, for aluminum (valence 3), N denotes the number of atoms and not the number of valence electrons (we take $2 \leq N \leq 21$). Systems with 7, 13, and 18 atoms are particularly stable, while clusters with 6, 9, 14, 15, and 16 atoms have smaller barriers. In contrast to sodium clusters, and with the exceptions of $N=7, 17$, and 18, the SCM-def and SCM-sph barriers are very similar.

Shell effects are more pronounced than in the case of sodium [about two times higher, as predicted by Eq. (19)].

TABLE III. Channel p with the lowest (first number) and the second lowest energy barrier (second number) in comparison to the observed potassium decay channels (Ref. 23).

N	SCM-sph	SCM-def	Expt.
20	3,4	3,4	3,7
21	4,3	3,6	3,7
22	3,2	3,6	3
23	3,4	3,4	3
24	2,3	3,4	3
25	3,4	3,4	3,5
26	2,3	4,3	3,9
27	2,3	4,3	3

These strong shell effects are responsible for the following features. First, the SCM critical numbers ($N_c = 21$ and 20 for SCM-sph and SCM-def, respectively) are much lower than the LDM value, due to the high stability of Al_{18}^{2+} . Second, the favorable decay channels predicted by the heat of reaction analysis⁴ are not those with the lowest barrier, except for $N=5, 7, 8, 10$, and 11. Finally, smaller clusters ($N < 14$) have significant barriers, with heights between 1 and 2 eV, while for $N < 5$ the LDM shows no barrier. The cluster Al_2^{2+} breaks spontaneously in two magic fragments.

Performing an all-electron *ab initio* calculation, Martínez and Vela²⁵ concluded that $p=1$ is the favored decay channel of small doubly charged aluminum clusters, with $2 < N < 6$, in good agreement with our SCM-sph results.

Let us consider the fission of doubly charged potassium clusters. Figure 4 presents our results in comparison with MD calculations done by Bréchnignac *et al.*²⁶ For potassium we use the jellium values of the LDM coefficients: $a_s = 0.54$ eV, $a_c = 0.17$ eV, $c = -0.082$, and $d_s' = 1.17$ bohr. The SCM-sph fission barriers are in good agreement with MD results for $7 \leq N \leq 10$, but for $N=11$ and 12 the barriers are overestimated. The system K_7^{2+} has no fission barrier in our calculations, while MD gives a 0.08-eV barrier. The magic cluster K_{10}^{2+} has the highest barrier in both cases.

Figure 4 also compares our barriers heights for the decay of doubly charged potassium clusters with an experimental estimate by Bréchnignac *et al.*²⁷ Although our barriers are, in general, lower than the experimental ones, the trend of the data is reasonably reproduced. There is a maximum at the magic cluster with $N=22$ and a minimum at $N=24$ due to the decay in two magic pieces: $K_{24}^{2+} \rightarrow K_{21}^{2+} + K_3^{2+}$. Using the experimental surface energy, our results would be shifted

TABLE IV. Critical numbers obtained by the LDM (N_c^{LDM}) and the SCM considering spherical (N_c^{sph}) and deformed (N_c^{def}) fragments. We use the LDM for the evaporation energy. Experimental values (N_c^{expt}) are taken from Ref. 10, for sodium and potassium and from Ref. 24 for aluminum.

Metal	N_c^{LDM}	N_c^{sph}	N_c^{def}	N_c^{expt}
Na^{2+}	28	28	27	27 ± 1
Al^{2+}	34	21	20	17 ± 1
K^{2+}	23	28	22	20 ± 1

TABLE V. Barrier height for several doubly charged sodium clusters given by several methods. CAP refers to the cylindrical averaged pseudopotential and MD to molecular dynamics.

Cluster	p	This work			Other work		Expt. ^c
		LDM	SCM-sph	SCM-def	CAP ^a	MD ^b	
Na ₈ ²⁺	3	0	0.18	0.58	0.16	0.16	
Na ₁₀ ²⁺	3	0	0.76	0.92	0.67	0.71	
Na ₁₂ ²⁺	3	0.07	0.55	0.68	0.30	0.29	
Na ₁₈ ²⁺	3	0.37	0.34	0.53	0.50		
	9	0.57	0.22	0.23	0.52		
Na ₂₇ ²⁺	3	0.55	0.57	0.88			0.80

^aReference 30.

^bReference 21.

^cReference 11.

upward, approaching the experimental values (the surface energy is underestimated in both jellium and stabilized jellium models).

Table III presents the potassium decay channels observed experimentally by Bréchnignac *et al.*,²³ and the two channels with the lowest barrier obtained in the SCM. Our results are consistent with the data.

Table IV shows the critical numbers N_c , obtained with the SCM for the most favorable fission channel. For sodium and potassium, the LDM gives a very good prediction of N_c , but for aluminum this quantity is considerably overestimated. This is due to the importance of shell corrections for high-density metals. The SCM-def results are in very good agreement with experiment for all the analyzed systems, while SCM-sph exaggerates the critical numbers.

IV. COMPARISON WITH OTHER METHODS AND CONCLUSIONS

Let us comment on some of the other authors results. Garcias *et al.*²⁸ used the so-called Blocki shapes to describe the jellium background and solved the Kohn-Sham equations for the fusion processes Na₂₁⁺+Na₂₁⁺ and Na₂₁⁺+Na₃⁺. Koizumi and Sugano²⁹ studied the asymmetric decay of some doubly charged silver clusters, solving the Kohn-Sham equations for a deformed jellium background described by the so-called funny-hills parametrization. This family of shapes was proposed to study symmetric, or slightly asymmetric, fission of heavy nuclei, but is not adequate to describe the very asymmetric reactions that are typical of clusters (it exhibits a very deformed surface, thus overestimating the barrier height). Garcias *et al.* and Koizumi and Sugano called attention to the importance of shell effects on the fission barrier on the one hand and of the shape of the jellium background on the other.

Models that consider localized ions represent an improvement on the continuous background models. Montag and Reinhard³⁰ used the cylindrical averaged pseudopotential scheme (CAPS) model, where the ionic structure is included in a simplified way, to study the fission of doubly charged sodium clusters, with 10, 12, and 18 atoms. They concluded that the preferred channel is always Na₃⁺, although the system Na₁₈²⁺ has a good chance of breaking symmetrically.

Molecular dynamics, as considered in Ref. 21, goes beyond pseudopotential-averaging methods since the ions have full freedom to move.

Table V presents a compilation of theoretical and experimental results for barrier heights. We consider some magic channels reported in the literature. There is an overall agreement between our SCM results and the CAPS and MD results (exceptions are Na₈²⁺, $p=3$, for SCM-def only; Na₁₂²⁺, $p=3$; and Na₁₈²⁺, $p=9$).

The case Na₁₂²⁺ is particularly interesting since the energetically favorable fission channel consists of two magic daughters (Na₉⁺ and Na₃⁺). Our barrier height is almost twice that obtained by other authors. For Na₁₈²⁺, the symmetric ($p=9$) is clearly favored in comparison with the asymmetric channel ($p=3$), in contrast to CAPS results, where the two decay channels have a very similar barrier.

In summary, the SCM is able to reproduce, with reasonable accuracy, more exact Kohn-Sham calculations for deformed jellium and even some MD results. These agreements made us confident of the method and lead us to apply it to clusters fission in a systematic way. We reproduced well the critical number not only for doubly charged sodium and potassium clusters but also for doubly charged aluminum clusters. It is therefore interesting to apply the SCM to other nonalkali metals and to compare the results with experiment.³¹

We have seen that shell effects modify considerably the LDM barriers, especially for metals with high valence-electron density, and have confirmed the importance of fragment deformations in shaping the fission barriers, a feature that was already pointed out by Yannouleas and Landman.¹⁹

Finally, we remark that while most of experimental data are from hot clusters (with a typical temperature of about 500 K), all our calculations were made at zero temperature. Since the shell structure is reduced at finite temperatures,³² further studies including thermal effects are needed.

ACKNOWLEDGMENTS

This work has been partially supported by Praxis XXI Project No. 2/2.1/FIS/26/94. A.V. acknowledges financial support by the Praxis XXI program.

- ¹M. Brack, *Rev. Mod. Phys.* **65**, 677 (1993).
- ²J. P. Perdew, H. Q. Tran, and E. D. Smith, *Phys. Rev. B* **42**, 11 627 (1990).
- ³A. Vieira and C. Fiolhais, *Phys. Lett. A* **220**, 231 (1996).
- ⁴A. Vieira, M. Brajczewska, and C. Fiolhais, *Int. J. Quantum Chem.* **56**, 239 (1995).
- ⁵C. Fiolhais and A. Vieira, in *Collective Motions in Nuclear Dynamics*, Proceedings of the Predeal International Summer School, edited by A. Raduta, D. Delian, and I. Ursu (World Scientific, Singapore, 1995), p. 523.
- ⁶V. M. Strutinsky, *Nucl. Phys. A* **95**, 420 (1967); **122**, 1 (1968).
- ⁷A. Vieira and C. Fiolhais, *Z. Phys. D* **37**, 269 (1996).
- ⁸C. Yannouleas and U. Landman, *J. Phys. Chem.* **99**, 14 577 (1995).
- ⁹M. G. Mustafa, U. Mosel, and H. W. Schmitt, *Phys. Rev. C* **7**, 1519 (1973).
- ¹⁰U. Näher, S. Frank, N. Malinowski, U. Zimmermann, and T. P. Martin, *Z. Phys. D* **31**, 191 (1994).
- ¹¹C. Bréchnignac, Ph. Cahuzac, F. Carlier, and M. de Frutos, *Phys. Rev. Lett.* **64**, 2893 (1990).
- ¹²C. Bréchnignac, Ph. Cahuzac, F. Carlier, M. de Frutos, P. Garnier, and N. Kebaoli, *Phys. Rev. B* **53**, 1091 (1996).
- ¹³A. Vieira and C. Fiolhais, in *Proceedings of the International Symposium on Similarities and Differences Between Atomic Nuclei and Clusters*, edited by Y. Abe, I. Asai, S. M. Lee, and R. Yabana, (American Institute of Physics, New York, in press).
- ¹⁴C. Fiolhais and J. P. Perdew, *Phys. Rev. B* **45**, 6207 (1992).
- ¹⁵A. Kiejna, *Phys. Rev. B* **47**, 7361 (1993).
- ¹⁶M. Seidl and M. Brack, *Ann. Phys. (N.Y.)* **245**, 275 (1995).
- ¹⁷H. Koizumi, S. Sugano, and Y. Ishii, *Z. Phys. D* **28**, 223 (1993).
- ¹⁸M. Brajczewska, C. Fiolhais, and J. P. Perdew, *Int. J. Quantum Chem.* **27**, 249 (1993).
- ¹⁹C. Yannouleas and U. Landman, *Phys. Rev. B* **51**, 1902 (1995).
- ²⁰J. Maruhn and W. Greiner, *Z. Phys.* **251**, 431 (1972).
- ²¹R. N. Barnett, U. Landman, and G. Rajagopal, *Phys. Rev. Lett.* **67**, 3058 (1991).
- ²²A. Rigo, F. Garcias, J. A. Alonso, J. M. López, M. Barranco, A. Mañanes, and J. Németh, *Surf. Rev. Lett.* **3**, 617 (1996).
- ²³C. Bréchnignac and Ph. Cahuzac, *Surf. Rev. Lett.* **3**, 607 (1996).
- ²⁴M. J. Jarrold, J. E. Bower, and J. S. Kraus, *J. Chem. Phys.* **86**, 3876 (1987).
- ²⁵A. Martínez and A. Vela, *Phys. Rev. B* **49**, 17 464 (1994).
- ²⁶C. Bréchnignac, Ph. Cahuzac, F. Carlier, M. de Frutos, R. N. Barnett, and U. Landman, *Phys. Rev. Lett.* **72**, 1636 (1994).
- ²⁷C. Bréchnignac, Ph. Cahuzac, F. Carlier, and M. de Frutos, *Phys. Rev. B* **49**, 2825 (1994).
- ²⁸F. Garcias, A. Mañanes, J. M. López, J. A. Alonso, and M. Barranco, *Phys. Rev. B* **51**, 1897 (1995).
- ²⁹H. Koizumi and S. Sugano, *Phys. Rev. A* **51**, R886 (1995).
- ³⁰B. Montag and P. G. Reinhard, *Phys. Rev. B* **52**, 16 365 (1995).
- ³¹M. Heinebrodt, S. Frank, N. Malinowski, F. Tast, I. M. L. Billas, and T. P. Martin, *Z. Phys. D* **40**, 334 (1997).
- ³²O. Genzken and M. Brack, *Phys. Rev. Lett.* **67**, 3286 (1991); M. Brack and O. Genzken, *Z. Phys. D* **19**, 51 (1991); **21**, 65 (1991).